



Hepatic alveolar echinococcosis: Comparative computed tomography study between two Chinese and two European centres

Tilmann Graeter^{a,1}, Haihua Bao^{b,1}, Eric Delabrousse^{c,f}, Eleonore Brumpt^{c,f}, Rong Shi^a, Weixia Li^b, Yi Jiang^d, Julian Schmidberger^e, Wolfgang Kratzer^{e,*}, Wenya Liu^d, the XUUB consortium

^a Department of Diagnostic and Interventional Radiology, University Hospital Ulm, 89081 Ulm, Germany

^b Qinghai University, Qinghai University First Affiliated Hospital, Qinghai Province, 810001 Xining, PR China

^c WHO Collaborating Centre on Prevention and Treatment of Human Echinococcosis/National French Reference Centre for Echinococcosis, University Bourgogne Franche-Comté (UFC), 25030 Besançon, France

^d Xinjiang Medical University, First Affiliated Hospital, WHO Collaborating Centre on Prevention and Care Management of Echinococcosis, 830054 Urumqi, Xinjiang Uyghur Autonomous Region, PR China

^e Department of Internal Medicine I, University Hospital Ulm, 89081 Ulm, Germany

^f Besançon University Hospital, 25030 Besançon, France

ARTICLE INFO

Article history:

Received 15 April 2020

Received in revised form 29 April 2020

Accepted 30 April 2020

Keywords:

Alveolar echinococcosis

Intercontinental

Echinococcus multilocularis Ulm Classification for Computed Tomography (EMUC-CT)

Morphology

Evolution

ABSTRACT

The main endemic areas for alveolar echinococcosis (AE) are in Central Europe and Western China, and in >98% of cases, AE manifests in the liver. The aim of this work was to compare European and Chinese patient groups for number, size, and computed tomography (CT) appearance of hepatic AE lesions.

A total of 200 CT scans of patients with hepatic AE were evaluated by four blinded, experienced radiologists from two European (Besançon, Ulm) and two Chinese centres (Xining, Urumqi). In addition to noting the number, size, and localisation of the lesions, the radiologists evaluated morphological appearance using the *Echinococcus multilocularis* Ulm Classification – CT scheme. Chinese patients were younger than European patients (36.8 ± 13.2 vs. 63.5 ± 17.7 ; $p < 0.0001$) and had significantly larger lesions (120.4 ± 50.8 vs. 70.9 ± 39.8 ; $p < 0.0001$). The morphological appearance of the lesions on CT differed significantly between the two groups ($p < 0.05$), as did the number of lesions (2.6 ± 3.9 in European centres versus 3.8 ± 5.0 in Chinese centres; $p = 0.0062$).

Patient age and AE-related morphological manifestations differ between Europe and China, but the reasons for the differences are unknown.

© 2020 Published by Elsevier B.V. This is an open access article under the CC BY-NC-ND license (<http://creativecommons.org/licenses/by-nc-nd/4.0/>).

1. Introduction

Alveolar echinococcosis (AE) is a rare zoonosis caused by the larval stage of the fox tapeworm (*Echinococcus multilocularis*) (Eckert et al., 2001; Kern et al., 2017; Kantarci et al., 2012; Moro and Schantz, 2009). Frequently showing disseminated growth, AE resembles a malignant tumour in its appearance and destructive behaviour. In humans, AE may cause serious, potentially fatal

* Corresponding author at: Department of Internal Medicine I, University Hospital Ulm, Albert-Einstein-Allee 23, 89081 Ulm, Germany.

E-mail address: wolfgang.kratzer@uniklinik-ulm.de (W. Kratzer).

¹ Contributed equally.

illness (Eckert et al., 2001; Kern et al., 2017; Moro and Schantz, 2009; Eckert and Deplazes, 2004). It occurs predominantly in temperate-to-cold climate zones of the northern hemisphere, particularly across Central Europe, a large part of North and Central Asia, and some parts of North America (Eckert et al., 2001; Kern et al., 2017; Kern et al., 2003). Europe is the historical endemic region for AE, but since the 1980s, almost 90% of cases have occurred in western China (Vuitton et al., 2011).

Human infection with *Echinococcus multilocularis* is caused by ingestion of parasite eggs. High-risk groups for AE include dog and cat owners, who may become infected through close contact with their animals (Kern et al., 2004), and owning a dog is currently a major risk factor for contracting AE (Conraths et al., 2017). In endemic areas, farmers, forestry workers, and hunters have a higher risk of infection than do other occupational groups (Kern et al., 2004; Conraths et al., 2017). The current epidemiological picture for AE shows that the important main endemic areas for the disease are in Southern Germany, Northern Switzerland, Western Austria and Eastern France in Europe as well as in Western China (Baumann et al., 2019).

AE diagnosis remains a major clinical challenge. The case definition according to Brunetti et al. provides important recognised diagnostic criteria (Brunetti et al., 2010). Among available imaging techniques, the most investigated methods are ultrasonography, magnetic resonance imaging (MRI), and computed tomography (CT). Recognised AE classifications are available for ultrasonography and MRI (Kratzer et al., 2015; Kodama et al., 2003). The *Echinococcus multilocularis* Ulm classification for CT (EMUC-CT), newly developed by Graeter et al. (2016), offers the first description of different morphological types and patterns of AE liver lesions on CT (Graeter et al., 2016). Because of differences in health systems worldwide – especially between Europe and China – published studies have reported quite large regional differences, especially in AE lesion sizes. AE is often discovered by chance and very late because of the long incubation period. Therefore, imaging techniques can currently describe only point prevalence or morphological manifestations. It is possible that AE is diagnosed at earlier stages in Europe and later stages in China, but no studies have compared the two patient populations.

AE is rare, so multi-centre studies are required to accumulate sufficient data (Rath et al., 2017). To advance AE research, universities in European countries and China established a research network in 2016, the Xining–Urumqi–Ulm–Besançon (XUUB) project. The universities of Urumqi and Xining in western China and the universities of Ulm in Germany and Besançon in France have been leading centres in the research and treatment of AE for many years (see map, Fig. 1). These four institutions are each located in high-endemic areas for AE in their respective countries (Baumann et al., 2019).

The aim of the research network was to complete the first investigation and comparison of large AE patient datasets between Europe and China. For this purpose, we compared the number, size, and CT appearance of hepatic AE lesions between patient groups in these regions.

2. Materials and methods

2.1. Study design and inclusion and exclusion criteria

Retrospectively, we included the 50 most recent abdominal contrast-enhanced CT examinations ($N = 200$) at each centre, performed because of hepatic AE from 09/21/07 to 03/21/18. The number of cases was estimated after consultation with the

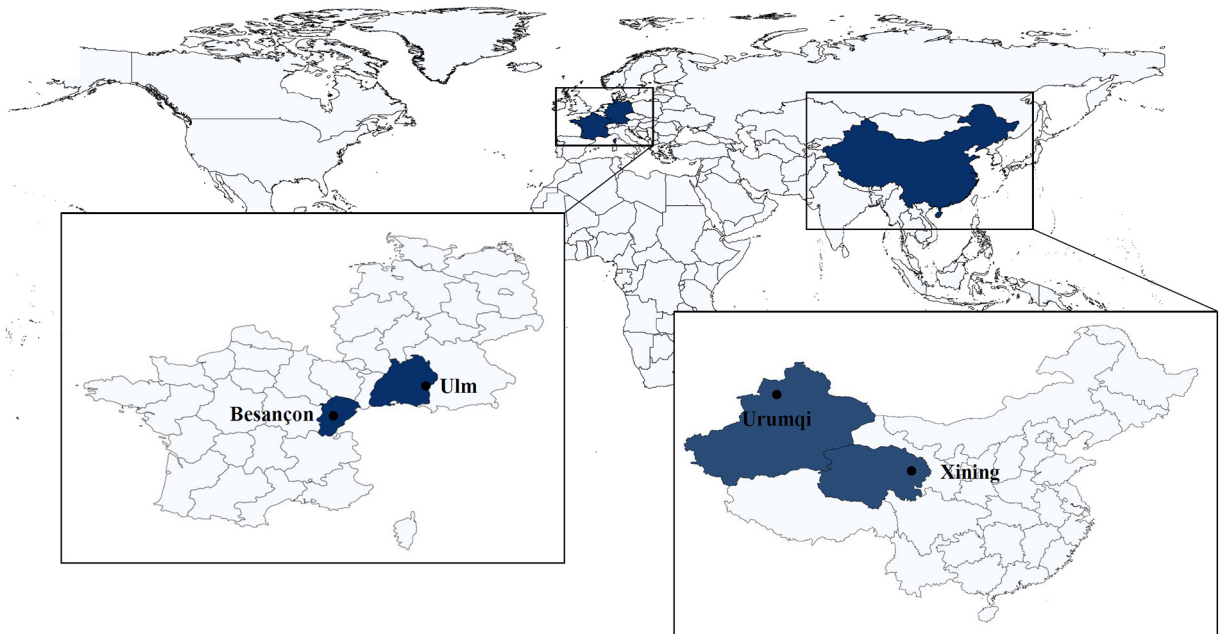


Fig. 1. Centre locations. The map shows the four centres in China and Europe: Xining in central China and Urumqi in the northwest of the country; Besançon in eastern France and Ulm lying at the southeastern border of the Swabian Alps on the border with Bavaria (especially created for this publication).

respective countries involved and the number of CT examinations in recent months. The previous clinical and imaging morphological findings had to have been classified as confirmed AE according to Brunetti et al.'s case definition (Brunetti et al., 2010). Antibody status, possible subsequent therapeutic strategies, and socioeconomic factors were not considered in the inclusion criteria.

2.2. Ethics approval and consent to participate

For German patients, the study was approved by the Institutional Review Board (IRB) of the Ulm University Hospital and conducted in accordance with the Declaration of Helsinki (ref. No. 409/15). Because of its retrospective design and pseudonymised evaluation of imaging, no ethics approval was necessary for France and China by the local Institutional Review Boards of the Universities Xining, Urumqi and Besançon regarding the national regulations. All data were analysed anonymously.

2.3. Examination and classification

The *Echinococcus Multilocularis* Ulm Classification for CT (EMUC-CT) provides a scheme for classifying the very different morphological appearances of hepatic alveolar echinococcosis (HAE) lesions. The classification of all HAE cases according to the EMUC-CT was carried out by the first reader from 09/04/18 to 14/04/2018. Only venous-phase CT scans were used to evaluate the lesions. The largest lesion within a liver was used to determine the primary morphological type, and all further evaluations in this study reference these. A local experienced radiologist at each of the four centres became the second reader for their own 50 cases and independently re-classified the local cases (Fig. 2). Criteria concerning the classification of the lesions, as well as further technical and disease-related information, were collected on a detailed report form. In addition to the essential patient data (sex and age), technical information included the basic technical modality of the CT scan. The following CT scanners were used in the different centres: Philips ICT, United UCT (Xining); CT-Discovery CT 750 HD, GE Healthcare (Urumqi); Biograph mCT-S (40), Siemens Healthcare (Ulm) and Biograph; Siemens; CTI; Knoxville, TN (Besançon).

The EMUC-CT classification distinguishes five primary morphological lesions: type I, diffuse infiltrating; type II, primarily circumscribed tumour-like; type III, primarily cystoid (two subtypes: type IIIa, intermediate; type IIIb, widespread); and type IV, small cystoid/metastatic; type V, mainly calcified. Subcriteria are given for types I–III. The classification also distinguishes six patterns of calcification: without calcifications, with a central calcification, or with feathery, focal, diffuse, or primarily edge calcifications (Fig. 3) (Graeter et al., 2016).

Disease-related information included the affected liver segments, number of lesions, overall dimensions of the lesions, and measurements of specific areas within them. The largest liver lesion was used to determine the primary morphological type and evaluated as the main lesion of the disease. Where appropriate, other primary morphological types present in smaller lesions were designated as 'second patterns'.

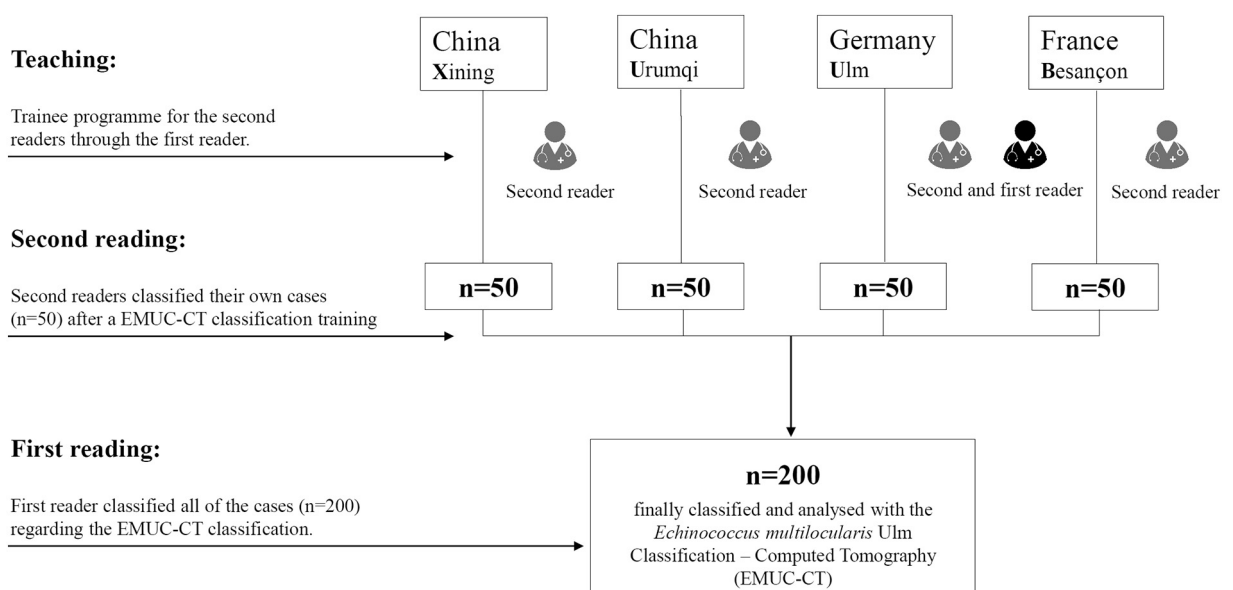


Fig. 2. Study design and course.

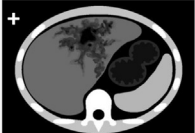
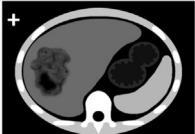
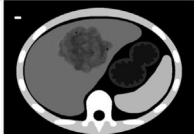
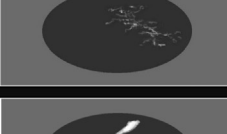
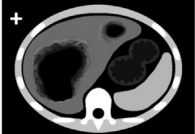
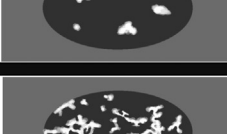
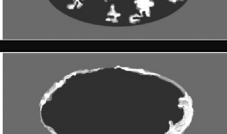
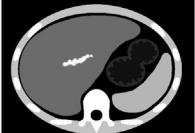
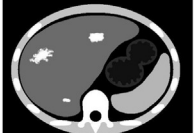
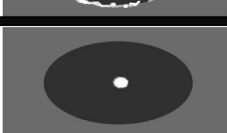
Primary morphology - Subcriteria			Pattern of calcification			
Type I Diffuse infiltrating + with cystoid portion - without cystoid portion	+		-		without calcifications	
Type II Primarily circumscribed, tumor-like + with cystoid portion - without cystoid portion	+		-		with feathery calcifications	
Type III Primarily cystoid: IIIa intermediate / IIIb widespread + with more solid portions at the edge - without more solid portions at the edge	+		-		with focal calcifications	
Type IV Small-cystoid, metastasis-like [⊗]	⊗				with diffuse calcifications	
Type V Mainly calcified					with calcifications primarily at the edge	
					with a central calcification [⊗]	

Fig. 3. Overview of the EMUC-CT classification. Left: Primary morphological types I–V and their subcriteria (applicable to types I, II, and III). Right: Patterns of calcification (EMUC-CT = *Echinococcus multilocularis* Ulm Classification for Computed Tomography). The two pillars of the classification are generally considered separately and can then in principle be freely combined. There are two exceptions: The pattern of calcification “with a central calcification” can occur only with primary morphology type IV[⊗], and primary morphology type V is not further characterised by a pattern of calcification.

2.4. Statistical analysis

Statistical analysis was performed using SAS Version 9.4 (SAS Institute Inc., Cary, NC, USA). First, a descriptive analysis of the data was performed with respect to the absolute and relative frequencies, as well as measures of central tendency and dispersion. The Shapiro-Wilk test was used to determine whether data were normally distributed. Pearson's chi-squared and the exact Fisher

Table 1
Patient characteristics.

	XUUB overall (N = 200)	Xining (n = 50)	Urumqi (n = 50)	Ulm (n = 50)	Besançon (n = 50)
Sex, n (%)					
Male	90 (45.0)	22 (44.0)	23 (46.0)	21 (42.0)	24 (48.0)
Female	110 (55.0)	28 (56.0)	27 (54.0)	29 (58.0)	26 (52.0)
Age, n (%)					
<18 years	8 (4.0)	6 (12.0)	2 (4.0)	0 (0.0)	0 (0.0)
18–40 years	59 (29.5)	20 (40.0)	26 (52.0)	8 (16.0)	5 (10.0)
41–60 years	66 (33.0)	24 (48.0)	18 (36.0)	12 (24.0)	12 (24.0)
61–80 years	50 (25.0)	0 (0.0)	4 (8.0)	26 (52.0)	20 (40.0)
>81 years	17 (8.5)	0 (0.0)	0 (0.0)	4 (8.0)	13 (26.0)
	Mean ± SD (min–max)				
Lesion size (mm)	95.6 ± 51.8 (11–261)	108.0 ± 53.0 (21–261)	132.7 ± 46.0 (36–253)	71.4 ± 46.39 (11–202)	70.4 ± 32.3 (13–173)
Number of lesions	3.2 ± 4.5 (1–29)	3.3 ± 5.3 (1–27)	1.8 ± 1.2 (1–6)	5.0 ± 6.5 (1–29)	2.7 ± 2.4 (1–12)
Age (years)	50.1 ± 20.5 (11–91)	35.5 ± 12.6 (11–55)	38.0 ± 13.9 (16–77)	61.3 ± 16.8 (18–85)	65.7 ± 18.3 (18–91)

test were used to evaluate differences in frequency between two variables. Differences in metric variables from the four centres were evaluated by post-hoc Tukey and Kruskal–Wallis tests based on an analysis of variance results. The level of significance was set at $\alpha = 0.05$, and $p < 0.05$ was considered significant with a 5% probability of error. All tests were performed on both sides.

3. Results

3.1. Sex proportion

The patient group ($n = 200$) across Xining ($n = 50$), Urumqi ($n = 50$), Ulm ($n = 50$), and Besançon ($n = 50$) had a pre-dominance of women at 110/200 (55%) (Table 1).

3.2. Age distribution

The European and Chinese patient populations differed significantly in age (63.5 ± 17.7 vs. 36.8 ± 13.2 ; $p < 0.0001$) (Table 1). The mean age of the patients in the two European centres (65.7 ± 18.3 years for Besançon and 61.3 ± 16.8 years for Ulm; overall mean, 63.5 years) was higher than in the two Chinese centres (38.0 ± 13.9 years for Urumqi and 35.5 ± 12.6 years for Xining; overall mean, 36.8 years; $\chi^2 = 87.98$; $p < 0.0001$).

3.3. Size of the largest space-occupying lesion

Lesion size also differed significantly between the European and Chinese patient populations (70.9 ± 39.8 vs. 120.4 ± 50.8 ; $p < 0.0001$). The mean size of the largest space-occupying lesion in all centres was 95.6 ± 51.8 mm. Lesions were smaller in Europe, with a mean measurement of 70.4 ± 32.3 mm for Besançon and 71.4 ± 46.4 mm for Ulm compared to 108.0 ± 53.0 mm for Xining and 132.7 ± 46.0 mm for Urumqi ($\chi^2 = 54.45$; $p < 0.0001$; Table 1).

3.4. Distribution of CT morphological patterns

The number of lesions differed significantly between the European and Chinese centres (2.6 ± 3.9 in Europe versus 3.8 ± 5.0 in China; $p = 0.0062$), but in a mixed pattern of high and low numbers in each region. The minimum was 1.8 ± 1.2 at Urumqi and the maximum was 5.0 ± 6.5 at Ulm (Table 1). Taking the cases from all centres, the frequencies of the primary morphological lesions decreased from type I to type V. However, the distribution of the primary morphology of the largest lesion was not the same in the European and Chinese centres (Table 2).

Type I was by far the most common type in the European centres, accounting for 50% of the primary lesions (28 [56.0%] for Besançon and 22 [44.0%] for Ulm) versus 35% of primary lesions in China. Type II was the second most common in Europe, with 12 (24.0%) in both centres. In Xining, type I and II frequencies were similar (18 [36.0%] and 17 [34.0%] cases, respectively). In contrast, type II dominated in Urumqi (26 [52.0%] cases compared to 17 [34.0%] type I cases). Taking the two localities together, type II was the most prevalent in the Chinese centres overall, accounting for 43% of cases, compared to 24% in Europe.

Type III (IIIa and IIIb combined) was identified much more often in China (20% vs. 7% in Europe), occurring in 13 (26.0%) cases in Xining and 7 (14.0%) in Urumqi, compared to 4 (8.0%) in Ulm and 3 (6.0%) in Besançon. Type IV accounted for 15 (15%) of the largest lesions in Europe and only 2 (2%) in China, where it was identified in only 2 (4.0%) cases in Xining and none in Urumqi. In

Table 2
Primary morphological types classified according to the EMUC-CT.

	N (%)				
	XUUB overall (N = 200)	Xining (n = 50)	Urumqi (n = 50)	Ulm (n = 50)	Besançon (n = 50)
Type I	85 (42.5)	18 (36.0)	17 (34.0)	22 (44.0)	28 (56.0)
With cystoid portion	55 (64.7)	13 (72.2)	13 (76.5)	11 (50.0)	18 (64.3)
Without cystoid portion	30 (35.3)	5 (27.8)	4 (23.5)	11 (50.0)	10 (35.7)
Type II	67 (33.5)	17 (34.0)	26 (52.0)	12 (24.0)	12 (24.0)
With cystoid portion	55 (82.1)	13 (76.5)	22 (84.6)	10 (83.3)	10 (83.3)
Without cystoid portion	12 (17.9)	4 (23.5)	4 (15.4)	2 (16.7)	2 (16.7)
Type III	27 (13.5)	13 (26.0)	7 (14.0)	4 (8.0)	3 (6.0)
With more solid portions at the edge	23 (85.2)	11 (84.6)	6 (85.7)	4 (100.0)	2 (66.7)
Without more solid portions at the edge	4 (14.8)	2 (15.4)	1 (14.3)	0 (0.0)	1 (33.3)
Type IIIa	8 (4.0)	2 (4.0)	1 (2.0)	2 (4.0)	3 (6.0)
With more solid portions at the edge	7 (87.5)	0 (0.0)	0 (0.0)	0 (0.0)	2 (66.7)
Without more solid portions at the edge	1 (12.5)	2 (100.0)	1 (100.0)	2 (100.0)	1 (33.3)
Type IIIb	19 (9.5)	11 (22.0)	6 (12.0)	2 (4.0)	0 (0.0)
With more solid portions at the edge	16 (84.2)	9 (81.8)	5 (83.3)	0 (0.0)	0 (0.0)
Without more solid portions at the edge	3 (15.8)	2 (18.2)	1 (16.7)	2 (100.0)	0 (0.0)
Type IV	17 (8.5)	2 (4.0)	0 (0.0)	9 (18.0)	6 (12.0%)
Type V	4 (2.0)	0 (0.0)	0 (0.0)	3 (6.0)	1 (2.0%)

contrast, it was found in 6 (12.0%) of the largest lesions in Besançon and 9 (18.0%) in Ulm. Type V was not identified in China and was found in only very small numbers in Europe (3 [6.0%] in Ulm and 1 [2.0%] in Besançon), accounting for 4% of the European patient group.

Thus, patients at the European and Chinese centres differed significantly in the distribution of type II (Europe, $n = 24$ [24.0%] vs. China, $n = 43$ [43.0%]; $\chi^2 = 8,10$; $p = 0.0044$) and type III patterns (Europe, $n = 7$ [7.0%] vs. China, $n = 20$ [20.0%]; $\chi^2 = 7,24$; $p = 0.0071$).

We also find significant difference in the distribution of type I (Europe, $n = 50$ [50.0%] vs. China, $n = 35$ [35.0%]; $\chi^2 = 4,60$; $p = 0.0319$) and type IV (Europe, $n = 15$ [15.0%] vs. China, $n = 2$ [2.0%]; Fisher's exact test: $p = 0.0015$). We found no significant differences in the distribution of type V (Europe, $n = 4$ [4.0%] vs. China, $n = 0$ [0.0%]; Fisher's exact test: $p = 0.1212$).

3.5. Lesion size according to CT morphological types

Mean lesion size and variance differed between CT morphological types and centres (Fig. 4). Type III lesions were particularly large, and type IV lesions showed the smallest mean lesion size and variance. They also were significantly smaller than all of the other lesions ($p < 0.05$).

3.6. Second pattern

The analysis also showed a second pattern of primary morphology in smaller lesions in 78/200 (39.0%) cases, with a different primary morphology from that of the main lesion. Table 3 gives the distribution of these lesions, designated as 'second patterns', at the different centres. Type IV was by far the most common second pattern, accounting for 56 (71.79%) cases, followed by 15 (19.23%) cases of the more rare type V. The distribution was similar across study centres.

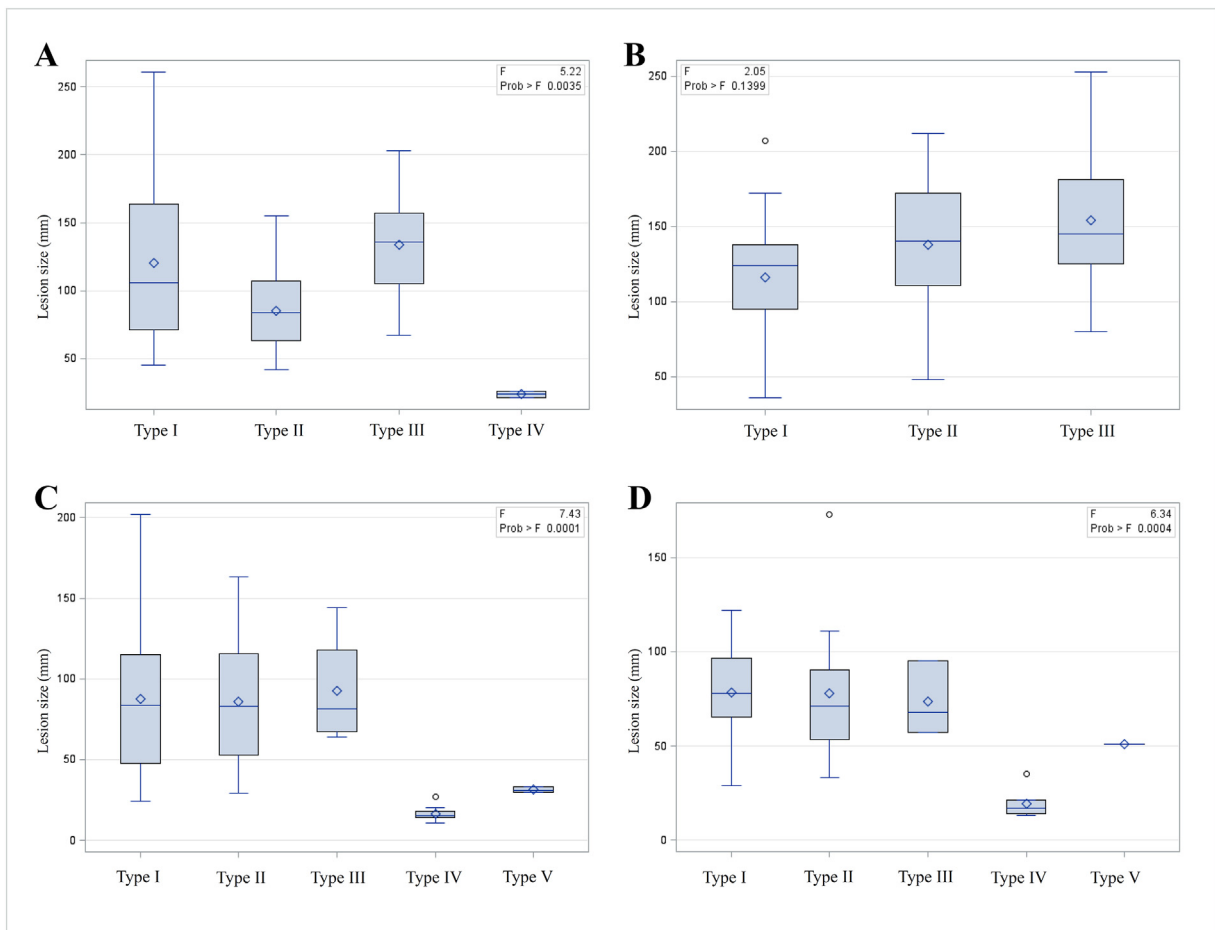


Fig. 4. Measures of central tendency and dispersion of the lesion size in the different centres. Box-plots showing measures of central tendency and dispersion of the lesion size, according to the EMUC-CT primary morphological types and centres. A: Xining, China; B: Urumqi, China; C: Ulm, Germany; D: Besançon, France.

Table 3
Morphological types found in additional lesions ('second patterns') stratified according to centre.

	N (%)				
	XUUB overall (N = 200)	Xining (n = 50)	Urumqi (n = 50)	Ulm (n = 50)	Besançon (n = 50)
Type I	2 (2.6)	1 (5.9)	0 (0.0)	0 (0.0)	1 (4.4)
Type II	3 (3.9)	0 (0.0)	0 (0.0)	3 (16.7)	0 (0.0)
Type III	2 (2.6)	1 (5.9)	0 (0.0)	1 (5.6)	0 (0.0)
Type IV	56 (71.8)	11 (64.7)	17 (85.0)	11 (61.1)	17 (73.9)
Type V	15 (19.2)	4 (23.5)	3 (15.0)	3 (16.7)	5 (21.7)
Overall	78 (39.0)	17 (34.0)	20 (40.0)	18 (36.0)	23 (46.0)

3.7. Calcification pattern

The six calcification patterns, which constitute the second pillar of the EMUC-CT scheme, showed a similar distribution in the largest lesions at all four centres. The 'without calcifications' pattern, however, was identified more often in European centres, with a trend towards 'feathery calcifications' and 'diffuse calcifications' in the two Chinese centres. Only a few cases had a 'central calcification', and all were exclusively in type IV lesions (from Xining, Ulm, and Besançon; Table 4).

4. Discussion

General information: In this study, we compared retrospectively collected CT data for a large group ($N = 200$) of patients with AE between the major endemic countries in Europe (Besançon, France; Ulm, Germany) and Asia (Xining and Urumqi, China). The results show significant differences between patients in Europe and China for lesion size and number and for patient age. The frequency and distribution of CT morphological patterns also differed by centre and region.

Age distribution: The large discrepancy in mean patient age between Chinese and European centres is particularly striking because the Chinese patients were younger. Several studies have already reported that echinococcosis occurs more often in children in western China than in other endemic regions of the world (Wang et al., 2006; Han et al., 2018; Cai et al., 2017). The high prevalence of endemic disease in young people indicates that infection occurs at an early age in the rural areas of north-western and western-central China, where stray dogs and herding dogs are thought to be responsible for dissemination of *Echinococcus multilocularis* eggs (Yu et al., 2017).

Sex distribution: The study also shows that in the four study centres, AE patients were more often female. This result is in keeping with previous reports of a predominance of women in this patient population (Wang et al., 2006).

Size of the largest space-occupying lesion: Lesion sizes differed significantly between the European and Chinese groups and were significantly larger in patients from the Chinese centres. In Europe, AE is often an incidental finding in asymptomatic older patients during a routine health check. Studies from China confirm that quite large lesions are frequently detected in the Asian region because of late diagnosis (Qu et al., 2017). Patients in China commonly do not present for medical diagnosis and treatment until they are symptomatic, usually at a late stage, because of residence in remote rural areas (Bresson-Hadni et al., 2000; Yang et al., 2006). The pattern of more advanced lesions in younger patients in China and less advanced lesions in older patients in Europe may seem paradoxical. Possible explanations include the more frequent contact that children in China may have with infected dogs because of a pastoral lifestyle, higher environmental infection pressure, and heavier egg burden at the time of infection. However, more rapid disease progression in a relatively immature immune system in early life cannot be ruled out.

Distribution of CT morphological patterns: The distribution of CT morphological types in the largest lesion differed between the European and Chinese groups. The primary morphology of the main lesion was most commonly type I and least commonly type V across all centres. These results correspond to the frequency distribution found in the German population when establishing the EMUC-CT in 2016 (Graeter et al., 2016). However, the centres in Europe and China differed in their individual distribution of the different types of primary morphology: European centres had a clear predominance of type I over type II whereas the

Table 4
Calcification pattern according to XUUB centre.

	N (%)				
	XUUB overall (N = 200)	Xining (n = 50)	Urumqi (n = 50)	Ulm (n = 50)	Besançon (n = 50)
Without calcifications	22 (11.0)	2 (4.0)	1 (2.0)	12 (24.0)	7 (14.0)
With feathery calcifications	41 (20.5)	12 (24.0)	15 (30.0)	4 (8.0)	10 (20.0)
With diffuse calcifications	74 (37.0)	23 (46.0)	18 (36.0)	19 (38.0)	14 (28.0)
With focal calcifications	41 (20.5)	9 (18.0)	13 (26.0)	9 (18.0)	10 (20.0)
With calcifications primarily at the edge	13 (6.5)	3 (6.0)	3 (6.0)	2 (4.0)	5 (10.0)
With a central calcification	5 (2.5)	1 (2.0)	0 (0.0)	1 (2.0)	3 (6.0)
No classification of type V	4 (2.0)	0 (0.0)	0 (0.0)	3 (6.0)	1 (2.0)

occurrence of these types was equal in Xining and type II showed predominance over type I in Urumqi. Type III, with strikingly large lesions, was more common at the two Chinese centres than in Europe. However, we also found significant differences in prevalence between Type II and Type III patterns in the European and Chinese patient groups. Type IV was seldom the main lesion, yet it was found with some regularity and almost exclusively in both European centres. Furthermore, it was by far the most common second pattern in patient populations from both regions. Type V was identified as the main lesion only among patients from the European centres and in very small numbers. So far, published descriptions of distributions of different CT morphological AE types are scant. It is possible that different stages explain the different types.

Calcification pattern: The distribution of the six calcification patterns that form the second pillar of the EMUC-CT was relatively similar at all centres. The pattern 'without calcifications' was detectably more common in the European centres, and the patterns 'feathery calcifications' and 'diffuse calcifications' tended to be more frequent in the two Chinese centres. For AE at least, calcification is reported to become more obvious as the disease progresses (Hosch et al., 2007). CT alone does not provide the entire information about the viability of the lesions, even in the case of highly calcified lesions. However, the strength of calcification is particularly important as a progression parameter because increasing calcification can be a sign of increasing lesion regression or of rapid, strong inflammatory reaction. Current studies on the strength of calcifications show, viewed the other way around, that especially low calcified lesions are associated with highest PET activity (Brumpton et al., 2019). Each imaging modality offers its specific advantages also for estimating the activity of AE lesions. For example, in MRI this would be the presence of the small alveoli (Azizi et al., 2015). MRI, however, in contrast to CT can only provide insufficient information on the calcification of a lesion.

Given the retrospective and purely descriptive nature of this study, it has several limitations. Among these are different imaging preferences and opportunities between the countries, as there were differences and a wide dispersion of imaging rates in the recruitment period. This factor must be considered as a possible confounder.

Nevertheless, this work provides a first holistic multicentric overview of the CT-based AE liver lesion morphology in Europe and China, using a classification system that allowed for direct comparison. The study design does not allow direct conclusions as to why the proportion of CT types, lesion size, and mean patient age differed between China and Europe. Further research should address these and other questions.

5. Conclusions

This study comparing patients with AE in Europe and China raises many questions and leaves open many possibilities for interpretation. Different lesion sizes with more extended liver infestations in China, as well as difference in mean ages and the differential distribution of CT morphological types between regions, raises the question of whether patients in Europe might have been at earlier stages of disease. In particular, there is a question of whether the type IV pattern could be the initial form of a lesion: these lesions were small and presented as a main lesion in the European group while at the same time representing the most common second pattern across centres. It is possible that these type IV lesions evolve into different types, but these questions need to be investigated in further multicentre studies.

Declaration of competing interest

All the authors declare that there is no conflict of interest.

Acknowledgements

We thank the World Health Organization Informal Working Group on Echinococcosis (WHO-IWGE), especially Dominique A. Vuitton, for initiating the XUUB cooperation.

Funding

The study was supported by a German Research Foundation (DFG)-funded project called "Establishment of a national database for alveolar echinococcosis" (Ref. No. KA 4356/3-1) and "Implementation of interfaces for the standardization of national database systems for alveolar echinococcosis and its transformation processes" (Ref. No. KR 5204/1-2); Natural Science Foundation of China (NSFC), 81260232, Multiple imaging study of the Hepatic Alveolar Echinococcosis after albendazole treatment; the Qinghai Science & Technology Department (Ref. No. 2017-SF-158); and the Müller Holding Ltd. & Co. KG Ulm.

Members of the consortium, by centre and alphabetically within centre listing

Besançon, France: Anne-Pauline Bellanger, Oleg Blagosklonov, Solange Bresson-Hadni, Florent Demonmerot, Frederic Grenouillet, Bruno Heyd, Jenny Knapp, Stephane Koch, Laurence Millon, Damien Montange, Josephine Moreau, Carine Richou, Celia Turco, Claire Vanlemmens, Dominique A Vuitton, Lucine Vuitton.

Ulm, Germany: Thomas FE Barth, Sven Baumann, Ambros J Beer, Meinrad Beer, Hartmut Döhner, Iris Fischer, Hans-Jürgen Groß, Beate Gruener, Doris Henne-Bruns, Andreas Hillenbrand, Silke Kapp-Schwörer, Katharina Klein, Patrycja Schlingeloff, Steffen Stenger, Frauke Theis.

Urumqi, China: Renyong Lin, Yingmei Shao, Aji Tuerganaili, Jian Wang, Hao Wen, Wenbao Zhang.

Xining, China: Yanling Bai, Jiayuan Cao, Haining Fan, Yingli Kang, Ren Li, Haijiu Wang, Xiaoping Wang, Shengbao Wen, Yousen Wu, Guixiu Yin, Wang Zhixin.

References

- Azizi, A., Blagosklonov, O., Lounis, A., Berthet, L., Vuitton, D.A., Bresson-Hadni, S., et al., 2015. Alveolar echinococcosis: correlation between hepatic MRI findings and FDG-PET/CT metabolic activity. *Abdom. Imaging* 40, 56–63.
- Baumann, S., Shi, R., Liu, W., Bao, H., Schmidberger, J., Kratzer, W., et al., 2019. Worldwide literature on epidemiology of human alveolar echinococcosis: a systematic review of research published in the twenty-first century. *Infection* 47, 703–727.
- Bresson-Hadni, S., Vuitton, D.A., Bartholomot, B., Heyd, B., Godart, D., Meyer, J.P., et al., 2000. A twenty-year history of alveolar echinococcosis: analysis of a series of 117 patients from eastern France. *Eur. J. Gastroenterol. Hepatol.* 12, 327–336.
- Brumpt, E., Blagosklonov, O., Calame, P., Bresson-Hadni, S., Vuitton, D.A., Delabrousse, E., 2019. AE hepatic lesions: correlation between calcifications at CT and FDG-PET/CT metabolic activity. *Infection* 47, 955–960.
- Brunetti, E., Kern, P., Vuitton, D.A., Writing Panel for the WHO-IWGE, 2010. Expert consensus for the diagnosis and treatment of cystic and alveolar echinococcosis in humans. *Acta Trop.* 114, 1–16.
- Cai, H., Guan, Y., Ma, X., Wang, L., Wang, H., Su, G., et al., 2017. Epidemiology of echinococcosis among schoolchildren in Golog Tibetan Autonomous Prefecture, Qinghai, China. *Am J Trop Med Hyg* 96, 674–679.
- Conraths, F.J., Probst, C., Possenti, A., Boufana, B., Saulle, R., La Torre, G., et al., 2017. Potential risk factors associated with human alveolar echinococcosis: systematic review and meta-analysis. *PLoS Negl. Trop. Dis.* 11, e0005807.
- Eckert, J., Deplazes, P., 2004. Biological, epidemiological, and clinical aspects of echinococcosis, a zoonosis of increasing concern. *Clin. Microbiol. Rev.* 17, 107–135.
- Eckert, J., Gemmell, M.A., Meslin, F.X., Pawloski, Z.S., 2001. WHO/OIE Manual on Echinococcosis in Humans and Animals: A Public Health Problem of Global Concern. World Organization for Animal Health, Paris.
- Graeter, T., Kratzer, W., Oeztuerk, S., Haenle, M.M., Mason, R.A., Hillenbrand, A., et al., 2016. Proposal of computed tomography classification for hepatic alveolar echinococcosis. *World J. Gastroenterol.* 22, 3621–3631.
- Han, X.M., Cai, Q.G., Wang, W., Zhang, Q., Wang, Y.S., 2018. Childhood suffering: hyper endemic echinococcosis in Qinghai-Tibetan primary school students, China. *Infect Dis Poverty* 7, 71.
- Hosch, W., Stojkovic, M., Jänisch, T., Kauffmann, G.W., Junghanss, T., 2007. The role of calcification for staging cystic echinococcosis (CE). *Eur. Radiol.* 17, 2538–2545.
- Kantarci, M., Bayraktutan, U., Karabulut, N., Aydinli, B., Ogul, H., Yuce, I., et al., 2012. Alveolar echinococcosis: spectrum of findings at cross-sectional imaging. *Radiographics* 32, 2053–2070.
- Kern, P., Bardonnet, K., Renner, E., Auer, H., Pawlowski, Z., Ammann, R.W., et al., 2003. European echinococcosis registry: human alveolar echinococcosis, Europe, 1982–2000. *Emerg. Infect. Dis.* 9, 343–349.
- Kern, P., Ammon, A., Kron, M., Sinn, G., Sander, S., Petersen, L.R., et al., 2004. Risk factors for alveolar echinococcosis in humans. *Emerg. Infect. Dis.* 10, 2088–2093.
- Kern, P., Menezes da Silva, A., Akhan, O., Müllhaupt, B., Vizcaychipi, K.A., Budke, C., et al., 2017. The echinococcoses: diagnosis, clinical management and burden of disease. *Adv. Parasitol.* 96, 259–369.
- Kodama, Y., Fujita, N., Shimizu, T., Endo, H., Nambu, T., Sato, N., et al., 2003. Alveolar echinococcosis: MR findings in the liver. *Radiology* 228, 172–177.
- Kratzer, W., Gruener, B., Kaltenbach, T.E., Ansari-Bitzenberger, S., Kern, P., Fuchs, M., et al., 2015. Proposal of an ultrasonographic classification for hepatic alveolar echinococcosis: echinococcosis multilocularis Ulm classification-ultrasound. *World J. Gastroenterol.* 21, 12392–12402.
- Moro, P., Schantz, P.M., 2009. Echinococcosis: a review. *Int. J. Infect. Dis.* 13, 125–133.
- Qu, B., Guo, L., Sheng, G., Yu, F., Chen, G., Wang, Y., et al., 2017. Management of advanced hepatic alveolar echinococcosis: report of 42 cases. *Am J Trop Med Hyg* 96, 680–685.
- Rath, A., Salamon, V., Peixoto, S., Hivert, V., Laville, M., Segrestin, B., et al., 2017. A systematic literature review of evidence-based clinical practice for rare diseases: what are the perceived and real barriers for improving the evidence and how can they be overcome? *Trials* 18, 556.
- Vuitton, D.A., Wang, Q., Zhou, H.X., Raoul, F., Knapp, J., Bresson-Hadni, S., et al., 2011. A historical view of alveolar echinococcosis, 160 years after the discovery of the first case in humans: part 1. What have we learnt on the distribution of the disease and on its parasitic agent. *Chin. Med. J.* 124, 2943–2953.
- Wang, Q., Qiu, J., Yang, W., Schantz, P.M., Raoul, F., Craig, P.S., et al., 2006. Socioeconomic and behavior risk factors of human alveolar echinococcosis in Tibetan communities in Sichuan, People's Republic of China. *Am J Trop Med Hyg* 74, 856–862.
- Yang, Y.R., Williams, G.M., Craig, P.S., Sun, T., Yang, S.K., Cheng, L., et al., 2006. Hospital and community surveys reveal the severe public health problem and socio-economic impact of human echinococcosis in Ningxia Hui Autonomous Region, China. *Tropical Med. Int. Health* 11, 880–888.
- Yu, Q., Xiao, N., Yang, S.J., Han, S., 2017. Deworming of stray dogs and wild canines with praziquantel-laced baits delivered by an unmanned aerial vehicle in areas highly endemic for echinococcosis in China. *Infect Dis Poverty* 6, 117.